

## The Structural Distortion of the Anti-perovskite Nitride $\text{Ca}_3\text{AsN}$

MING Y. CHERN AND F. J. DiSALVO\*

*Department of Chemistry, Cornell University, Ithaca, New York 14853*

J. B. PARISE

*Mineral Physics Institute, State University of New York at Stony Brook, Stony Brook, New York 11794*

AND JOYCE A. GOLDSTONE

*LANSCE, Los Alamos National Laboratory, Los Alamos, New Mexico 87545*

Received May 9, 1991

The structure of the distorted anti-perovskite nitride  $\text{Ca}_3\text{AsN}$  has been studied both by neutron powder diffraction at 305 and 15 K and by X-ray powder diffraction at room temperature.  $\text{Ca}_3\text{AsN}$  is distorted to an orthorhombic cell with  $a$  and  $b \sim \sqrt{2} a'$  and  $c \sim 2a'$ , where  $a'$  is the lattice constant of the ideal undistorted cubic anti-perovskite. The distortion is produced by tilting of octahedra of  $\text{Ca}_6\text{N}$  and results in six short and six long bond distances of the twelfefold coordinated As atom by Ca atoms. © 1992 Academic Press, Inc.

### Introduction

Structural distortions of cubic perovskites of the formula  $ABX_3$ , where the cation  $A$  is coordinated by twelve  $X$  anions, and the cation  $B$  is in an octahedral site formed by six  $X$  anions, to structures of lower symmetry is commonly seen. Although the distortion can be very subtle and complicated, most of the distortions can be broken up into several simple components (1): (i) displacements of the cations, (ii) tilting of the anion octahedra, and (iii) distortions of the octahedra. For example,  $\text{BaTiO}_3$  is cubic at high temperatures, but, when

cooled below 393 K it undergoes a structural phase transition to a tetragonal phase with the  $\text{Ba}^{2+}$  and  $\text{Ti}^{4+}$  cations displaced along a cubic [001] direction relative to the  $\text{O}^{2-}$  anions (2). On further cooling, it changes structure again to an orthorhombic phase at 273 K and a rhombohedral phase below 183 K, in which the direction of cation displacements become parallel to [110] and [111], respectively (2). As another example,  $\text{SrTiO}_3$  has a structural phase transition from cubic to tetragonal when cooled below 195 K with the titanium-centered oxygen octahedra along the  $c$ -axis tilting alternately in opposite directions about that axis (3). In  $\text{CaTiO}_3$ , the displacement of the cations and the tilting of the anion octahedra occur si-

\* To whom correspondence should be addressed.

multaneously in the distorted structure (4). In  $\text{KCuF}_3$ , the  $\text{CuF}_6$  octahedra are elongated (distorted) along the corner-to-corner diameters on the waist, but both the cations, K and Cu, remain centered in their polyhedra (5).

Tilting of the anion octahedra, component (ii), often dominates the overall crystal structure. The effect of the tilting on the characteristics of the superlattice lines in diffraction patterns has been systematically studied, and all the 23 possible space groups due to this rotation of "rigid" octahedra have been classified by Glazer (6, 7). According to Glazer's scheme, three superscripts, +, -, and 0, are assigned to the three pseudo-cubic axes: A "+" sign means that all the octahedra along the axis have the same sense of rotation about that axis; a "-" sign means that the octahedra rotate alternately in opposite senses; and a "0" superscript means no tilt about the axis. Thus,  $\text{SrTiO}_3$  mentioned previously belongs to the system  $a^0b^0c^-$  or  $a^0a^0c^-$ , where the repeated  $a$  indicates equal tilt, which is zero in this case, about the  $a$ - and the  $b$ -axis.

The number of anti-perovskites  $M_3AB$ , where the positions of anion and the cation are reversed from normal perovskites, i.e.,  $A$  and  $B$  are anions and  $M$  is a cation, is much smaller than that of normal perovskites. However, anti-perovskites show the same tendency toward distortions as normal perovskites. In the course of searching for new ternary nitrides, we synthesized a series of anti-perovskites of the formula  $\text{Ca}_3\text{AN}$ , where  $A$  is a Group IV or a Group V element, of which  $\text{Ca}_3\text{AsN}$  and  $\text{Ca}_3\text{PN}$  are distorted from cubic and exhibit phase transitions at high temperatures (8). Interestingly, the above scheme, which works extremely well for the perovskites, can be applied equally well to the anti-perovskite  $\text{Ca}_3\text{AsN}$ . The purpose of this paper is to report the structure determination of  $\text{Ca}_3\text{AsN}$  by neutron and X-ray powder diffraction.

### Sample Preparation

Calcium nitride ( $\text{Ca}_3\text{N}_2$ ) was initially prepared by heating granular calcium ( $\sim 0.3 \times 0.3 \times 0.3 \text{ cm}^3$ ) in an  $\text{N}_2$  atmosphere at  $900^\circ\text{C}$ . A well-mixed stoichiometric mixture of  $\text{Ca}_3\text{N}_2$  and As was obtained by separately grinding the granular  $\text{Ca}_3\text{N}_2$  and As (also in a granular form) into fine powders and then mixing both together, in the ratio  $\text{Ca} : \text{As} = 3 : 1$ , in an alumina mortar and pestle. All the procedures were carried out in a dry box because  $\text{Ca}_3\text{N}_2$  and the product are moisture-sensitive.  $\text{Ca}_3\text{AsN}$  was subsequently prepared by heating a pressed pellet of the mixture in an alumina crucible under a flowing  $\text{N}_2$  atmosphere at  $100^\circ\text{C}/\text{hr}$  to  $1000^\circ\text{C}$  and held at that temperature for 2 days. The  $\text{N}_2$  gas (99.995%) was pre-purified by passing it through a column of finely divided copper powder at  $150^\circ\text{C}$  and then through a column of activated molecular sieves to remove traces of  $\text{O}_2$  and  $\text{H}_2\text{O}$ . Since at  $1000^\circ\text{C}$  the sample is very sensitive to oxidation by even minute amounts of  $\text{O}_2$  and  $\text{H}_2\text{O}$  remaining in the  $\text{N}_2$  gas, we further protected the sample by placing an alumina boat containing fine calcium nitride powder both before and after the sample in the alumina tube used to contain the  $\text{N}_2$  flow. The red-colored sample made by this method does not have any obvious contamination from oxide formation by visual inspection or by X-ray diffraction (see next section). Five pellets,  $\sim 1 \text{ g}$  each, are needed for the neutron diffraction, since the cross section for neutron diffraction is relatively small compared to X-ray scattering.

### X-ray and Neutron Powder Diffraction Measurements

X-ray powder diffraction data were collected at room temperature with a Scintag XDS 2000 diffractometer using copper  $K\alpha$  radiation over a  $2\theta$  range of  $5^\circ$  to  $95^\circ$  with a scanning interval of  $0.015^\circ$  and a count time

of 9 sec per interval. Both  $K\alpha_1$  and  $K\alpha_2$  lines were used for the structure refinement. The sample was loaded in an aluminum holder and covered with a 0.5 mil. thick layer of Mylar in a dry box to avoid air exposure. The Mylar sheet was supported by two semicircular disks standing perpendicular to the sample so that the absorption due to the Mylar is uniform and small over the whole  $2\theta$  range. The sample dimensions are such that over the whole  $2\theta$  range the X-ray beam is fully intercepted by the powdered sample.

A 5-g sample of freshly prepared sample of  $\text{Ca}_3\text{AsN}$  was packed into a standard vanadium "little finger" sample holder, fitted with an indium o-ring seal, in a dry box. Data were taken at 15 and 305 K on the neutron powder diffractometer (NPD) at the Manuel Lujan, Jr., Neutron Scattering Center (LANSCE) at the Los Alamos National Laboratory. The NPD has a flight path of 32 m and a resolution  $\Delta d/d$  of  $1 \times 10^{-3}$ . Data were collected in four detector banks, at approximately  $\pm 148^\circ$  and  $\pm 90^\circ$ , for about 24 and 18 hr at 305 and 15 K, respectively, at average proton currents on the spallation source of 50  $\mu\text{A}$ . Some of the diffraction

data collected in the 148 data banks are shown in Figs. 1 and 2.

### Unit Cell and Structure Determination

The unit cell was initially thought to be tetragonal. All the  $00l$  lines of the original cubic cell split into doublets in the X-ray diffraction patterns. Further, the calculated line positions, based on a tetragonal cell whose axes are all approximately doubled along the three axes of the cubic cell, fit the positions of the split peaks and the superlattice reflections very well. However, attempts to solve the distorted structure in tetragonal space groups were never satisfactory, even though all possible tetragonal space groups were tried. The only possibility left is that the unit cell is monoclinic with  $a$  being exactly equal to  $b$  and the angle  $\gamma$  between  $a$  and  $b$  being very close to  $90^\circ$  (see Fig. 6). Here, the  $c$ -axis is the unique axis for the monoclinic cell. It is on this latter assumption that the structure was refined successfully, but it is very difficult to detect the deviation of the angle  $\gamma$ ,  $89.95^\circ$  (see the discussion below), from  $90^\circ$ .

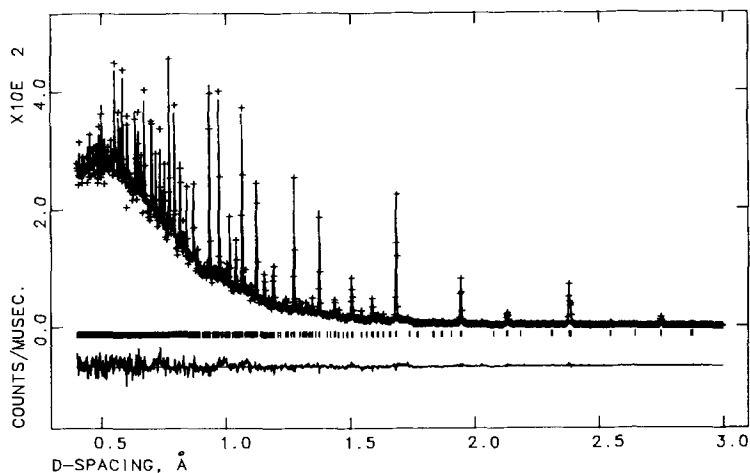


FIG. 1. Observed (+) and calculated (solid line) neutron TOF diffraction profiles from the  $148^\circ$  bank for  $\text{Ca}_3\text{AsN}$  at 305 K. The reflection markers and the difference profile are also shown.

Further examination of the superlattice reflections indicated that the monoclinic cell was C-centered so it can be reduced to a primitive orthorhombic cell. Two orthorhombic space groups,  $Pbn2_1$  (no. 33) and  $Pbnm$  (no. 62), are consistent with the reflection conditions observed:  $0kl$ ,  $k = 2n$ ;  $h0l$ ,  $h + l = 2n$ ;  $h00$ ,  $h = 2n$ ;  $0k0$ ,  $k = 2n$ ; and  $00l$ ,  $l = 2n$ . However, in addition to the above general conditions, we also found some special rules for the superlattice reflections with reference to the doubled pseudo-cubic cell: they are either of the type (a) odd-odd-even with  $h \neq k$ , or of the type (b) odd-odd-odd with  $h \neq l$  or  $k \neq l$ . For example, the 211 reflection of the orthorhombic cell, which is indexed as 311 or 131 (odd-odd-odd) on the doubled pseudo-cubic cell with  $h \neq l$  or  $k \neq l$ , is observed; the orthorhombic reflection 212, which becomes 312 or 132 (odd-odd-even) referred to the doubled cell with  $h \neq k$ , is also de-

tected. No superlattice reflections were observed other than those which are consistent with these special rules.

Glazer (6, 7) has analyzed the characteristics of the superlattice lines due to the tilting of the octahedra. Tilt " $c^+$ " can produce reflections of type (a), while tilts " $a^-$ " and " $b^-$ " produce type (b) reflections. To satisfy both the general conditions and the special rules, the space group  $Pbn2_1$  can be ruled out and the space group  $Pbnm$  is used with the tilt system  $a^-a^-c^+$  as the starting model for structure refinement. (The symmetry of the space group would have to be lowered to accommodate  $a^-b^-c^+$ .)

### Structure Refinement

Eight calcium, four calcium, four nitrogen, and four arsenic atoms are initially located at positions (8d), (4c), (4b), and (4a) of space group  $Pbnm$ , respectively,

---

Ca(1): (8d)	$\frac{3}{4} - \Delta_1, \frac{1}{4} + \Delta_2, \delta;$ $\frac{3}{4} + \Delta_1, \frac{3}{4} + \Delta_2, \delta;$ $\frac{1}{4} - \Delta_1, \frac{1}{4} - \Delta_2, -\delta;$ $\frac{1}{4} + \Delta_1, \frac{3}{4} - \Delta_2, -\delta;$	$\frac{3}{4} - \Delta_1, \frac{1}{4} + \Delta_2, \frac{1}{2} - \delta;$ $\frac{3}{4} + \Delta_1, \frac{3}{4} + \Delta_2, \frac{1}{2} - \delta;$ $\frac{1}{4} - \Delta_1, \frac{1}{4} - \Delta_2, \frac{1}{2} + \delta;$ $\frac{1}{4} + \Delta_1, \frac{3}{4} - \Delta_2, \frac{1}{2} + \delta.$
Ca(2): (4c)	$\gamma_1, \frac{1}{2} - \gamma_2, \frac{1}{4};$ $\frac{1}{2} - \gamma_1, -\gamma_2, \frac{1}{4};$	$-\gamma_1, \frac{1}{2} + \gamma_2, \frac{3}{4};$ $\frac{1}{2} + \gamma_1, \gamma_2, \frac{3}{4}.$
N: (4b)	$\frac{1}{2}, 0, 0;$ $0, \frac{1}{2}, 0;$	$\frac{1}{2}, 0, \frac{1}{2};$ $0, \frac{1}{2}, \frac{1}{2}.$
As: (4a)	$-\lambda_1, \lambda_2, \frac{1}{4};$ $\frac{1}{2} - \lambda_1, \frac{1}{2} - \lambda_2, \frac{3}{4};$	$\lambda_1, -\lambda_2, \frac{3}{4};$ $\frac{1}{2} + \lambda_1, \frac{1}{2} + \lambda_2, \frac{1}{4}.$

---

Here  $\Delta_1$ ,  $\Delta_2$ ,  $\delta$ ,  $\gamma_1$ ,  $\gamma_2$ ,  $\lambda_1$ , and  $\lambda_2$  are small fractions of the coordinates, on the order of 0.001, deviating from the ideal positions, e.g.  $\frac{3}{4}, \frac{1}{4}, 0; \frac{3}{4}, \frac{1}{4}, \frac{1}{2}; \dots$ ; etc. Rietveld profile analysis is used to refine those coordinates with the X-ray and neutron powder diffraction data separately, and the generalized crystal structure analysis system (GSAS) (9) was used. For the neutron data, the 85 variables refined include lattice constants, atomic coordinates and isotropic thermal

factors, and, in addition, a scale factor, four peak profile parameters ( $\alpha_1, \beta_1, \beta_2, \sigma_1$ ) (10), twelve Fourier background coefficients, and a diffractometer zero correction for each data bank. In the final refinement the  $x$ -coordinate of the As atom was fixed at the ideal value, 0, since its deviation from 0 is within 3 standard deviations. The refined results are shown in Tables I and II; the observed intensities along with the calculated profiles and the difference plot are represented in

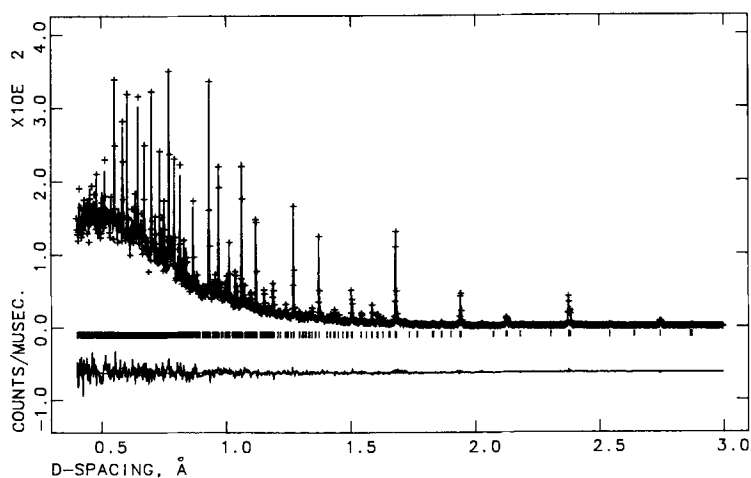


FIG. 2. Observed (+) and calculated (solid line) neutron TOF diffraction profiles from the 148° bank for  $\text{Ca}_3\text{AsN}$  at 15 K. The reflection markers and the difference profile are also shown.

TABLE I  
STRUCTURAL PARAMETERS AT 305 K DETERMINED FROM RIETVELD REFINEMENT  
OF NEUTRON POWDER DIFFRACTION DATA

Space group

*Pbnm*

Lattice constants

$$a = 6.7301(2) \text{ \AA}, b = 6.7246(2) \text{ \AA}, c = 9.5402(2) \text{ \AA}$$

Atomic coordinates

Atom	Symmetry position	x	y	z
Ca(1) <sup>a</sup>	(8d)	0.7211(5)	0.2821(5)	0.0174(2)
Ca(2)	(4c)	0.0310(4)	0.4947(7)	0.2500
N	(4b)	0.5000	0.0000	0.0000
As	(4a)	0.0000	0.0108(4)	0.2500

Deviations from the ideal sites

$$\Delta_1 = 0.0289, \Delta_2 = 0.0321, \delta = 0.0174, \gamma_1 = 0.0310, \gamma_2 = 0.0053, \lambda_1 = 0.0000, \lambda_2 = 0.0108$$

Isotropic thermal parameters

Atom	Symmetry position	$U(\times 10^2 \text{ \AA}^2)$
Ca(1)	(8d)	1.47(7)
Ca(2)	(4c)	1.8(1)
N	(4b)	0.9(1)
As	(4a)	1.35(8)

Residual factors

$$R_p = 4.6\%, R_{wp} = 6.9\%, \text{reduced } \chi^2 = 1.76 \text{ for 85 variables}$$

<sup>a</sup> Scattering amplitudes taken from Ref. (9).

TABLE II  
STRUCTURAL PARAMETERS AT 15 K DETERMINED FROM RIETVELD REFINEMENT  
OF NEUTRON POWDER DIFFRACTION DATA

Space group				
<i>Pbnm</i>				
Lattice constants				
$a = 6.7159(2) \text{ \AA}$ , $b = 6.7110(2) \text{ \AA}$ , $c = 9.5198(2) \text{ \AA}$				
Atomic coordinates				
Atom	Symmetry position	<i>x</i>	<i>y</i>	<i>z</i>
Ca(1)	(8 <i>d</i> )	0.7171(3)	0.2821(3)	0.0209(1)
Ca(2)	(4 <i>c</i> )	0.0404(3)	0.4942(4)	0.2500
N	(4 <i>b</i> )	0.5000	0.0000	0.0000
As	(4 <i>a</i> )	0.0000	0.0168(2)	0.2500
Deviations from the ideal sites				
$\Delta_1 = 0.0329$ , $\Delta_2 = 0.0321$ , $\delta = 0.0209$ , $\gamma_1 = 0.0399$ , $\gamma_2 = 0.0048$ , $\lambda_1 = 0.0000$ , $\lambda_2 = 0.0170$				
Anisotropic thermal parameters				
Atom	Symmetry position	$U(\times 10^2 \text{ \AA}^2)$		
Ca(1)	(8 <i>d</i> )	0.54(6)		
Ca(2)	(4 <i>c</i> )	0.57(7)		
N	(4 <i>b</i> )	0.53(6)		
As	(4 <i>a</i> )	0.42(5)		
Residual factors				
$R_p = 5.4\%$ , $R_{wp} = 8.3\%$ , reduced $\chi^2 = 1.57$ for 85 variables				

Figs. 1 and 2 for the 148° data bank at 305 and 15 K, respectively. Also, the region from 1.0 to 1.3 Å of the two figures are scaled up in Figs. 3 and 4 to clearly show the fit. For the X-ray data, the same variables were refined, but the peak profile parameters used were a combination of Gaussian and Lorentzian shapes (*GU*, *GV*, *GW*, *LX*, *LY*, and *LZ*) (11, 12), and the thermal parameters were fixed at the values refined from the neutron data. Otherwise a small nonphysical negative thermal parameter for the nitrogen atom with a slightly lower residual was obtained. This likely happens because X-ray diffraction is not sensitive to a light element such as nitrogen. The results are shown in Fig. 5 and Table III.

## Results and Discussion

The structure of  $\text{Ca}_3\text{AsN}$  is drawn in Fig. 6 with a view down the *c*-axis. The dotted lines outline the doubled cell which contains eight calcium octahedra before the tilting; the waists of the octahedra are at  $z = 0$  and  $z = \frac{1}{2}$ . When the  $c^+$  tilt occurs, the octahedra rotate to the positions shown by the solid lines, and the doubled cell becomes C-centered monoclinic so it can be reduced in volume by a factor of two to the orthorhombic cell outlined by the bold solid lines. The angle “ $\gamma$ ” of the monoclinic cell is equal to  $2 \sin^{-1}[b/(a^2 + b^2)^{1/2}] \sim 89.95^\circ$ —very close to  $90^\circ$ . The calcium atoms on the waists, Ca(1), move away from their ideal sites by

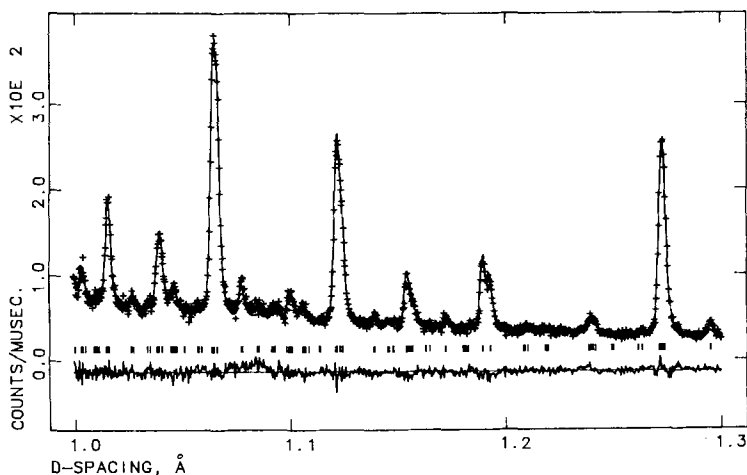


FIG. 3. Magnification of Fig. 1 from 1.0 to 1.3 Å.

a distance  $[(\Delta_1 \cdot a)^2 + (\Delta_2 \cdot b)^2]^{1/2} \sim 0.29 \text{ \AA}$  at room temperature due to the tilting. (See the last section for the coordinates of the Ca(1) atoms.) Note that the neighbors of a rotating octahedron in the  $ab$ -plane have to rotate about the  $c$ -axis in opposite directions because they are all "rigid". On the other hand, the  $+$  tilt requires that the octahedra above and below it have the same rotation. The other two tilts about the  $a'$  and  $b'$ -axis are indicated by the arrowed semicircles.

The two semicircles along the  $\alpha'$ -axis have opposite senses of rotation because of the  $-$  tilt, and so do the semicircles along the  $b'$ -axis. As a result, the Ca(1) atoms are also lifted up or pushed down the  $z$ -planes by a distance  $\delta \cdot c \sim 0.17 \text{ \AA}$ . The arrows on the tops of the octahedra indicate the movements of the Ca(2) atoms as a combined effect of the two equal  $-$  tilts, and the magnitude of the movements is equal to  $[(\gamma_1 \cdot a)^2 + (\gamma_2 \cdot b)^2]^{1/2} \sim 0.21 \text{ \AA}$ . In fact the

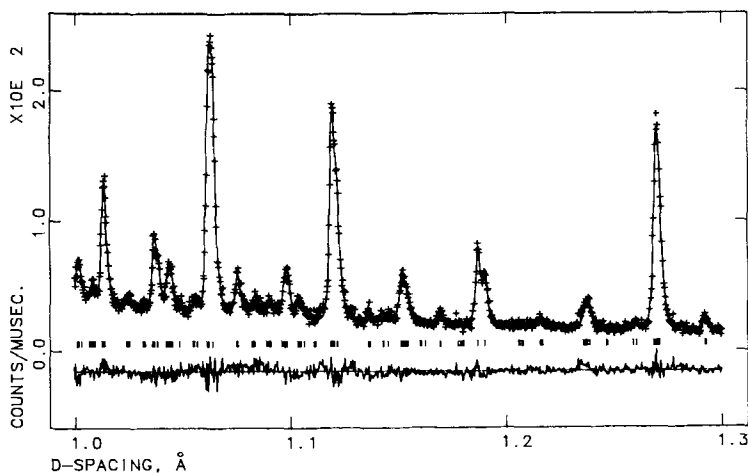


FIG. 4. Magnification of Fig. 2 from 1.0 to 1.3 Å.

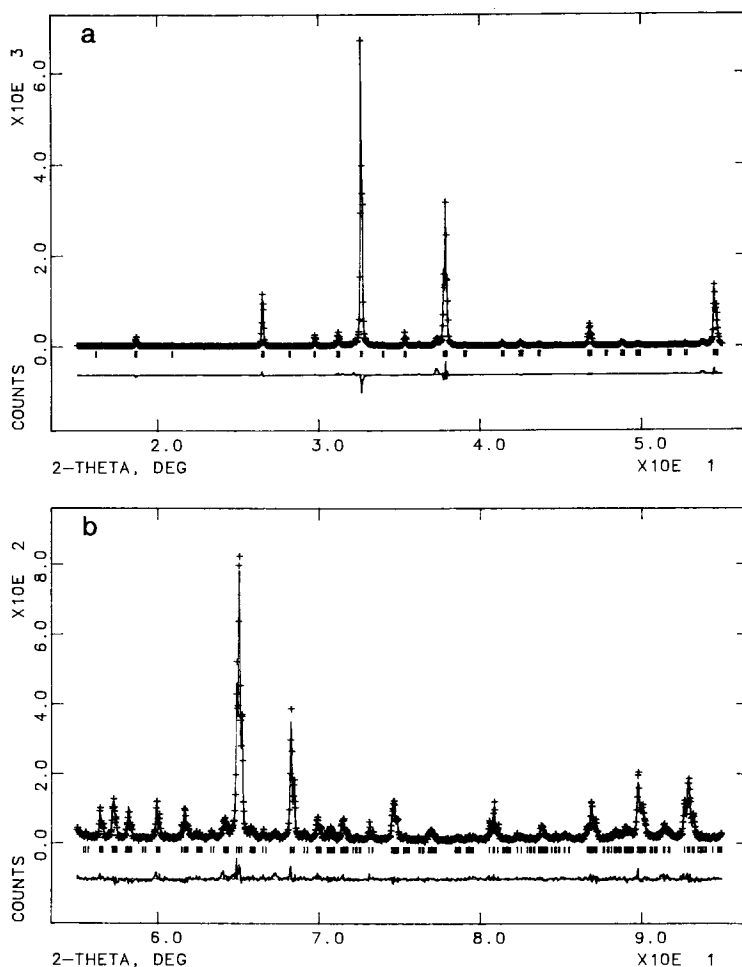


FIG. 5. Observed (+) and calculated (solid line) X-ray powder diffraction profiles for  $\text{Ca}_3\text{AsN}$  at room temperature. The reflection markers and the difference profile are also shown: (a)  $15^\circ$  to  $55^\circ$ , (b)  $55^\circ$  to  $95^\circ$ .

combination of the two – tilts is equivalent to a single tilt about the  $b$ -axis. One can verify from the symmetry of the pattern exhibited by these arrows that the space group should be  $Pbnm$ .

In this structure the calcium octahedra stay almost rigid since we find that the waists of the octahedra formed by the Ca(1) atoms are essentially square (i.e.,  $\Delta_1 \cdot a \sim \Delta_2 \cdot b$ ) and that the magnitude of the movements of the Ca(2) atoms is almost equal to square root two times the height of the Ca(1)

atoms above or below the  $z$ -planes (i.e.,  $[(\gamma_1 \cdot a)^2 + (\gamma_2 \cdot b)^2]^{1/2} \sim \sqrt{2} \delta \cdot c$ ) as expected from the behavior of a rigid octahedron. Since the octahedra are almost regular and the tilt angles are small, the tilt angles can be estimated according to the formula,

$$\phi \sim \sin^{-1}[\sqrt{2} (\Delta_1 \cdot a)/(c/4)],$$

$$\omega \sim \sin^{-1}[(\delta \cdot c)/(c/4)],$$

$$\text{and } \varphi \sim \sin^{-1}[(\gamma_1 \cdot a)/(c/4)],$$

TABLE III  
STRUCTURAL PARAMETERS AT ROOM TEMPERATURE DETERMINED FROM RIETVELD REFINEMENT  
OF X-RAY POWDER DIFFRACTION DATA

Space group				
<i>Pbnm</i>				
Lattice constants				
$a = 6.7250(2) \text{ \AA}$ , $b = 6.7198(2) \text{ \AA}$ , $c = 9.5335(1) \text{ \AA}$				
Atomic coordinates				
Atom	Symmetry position	<i>x</i>	<i>y</i>	<i>z</i>
Ca(1)	(8 <i>d</i> )	0.721(1)	0.279(1)	0.0171(4)
Ca(2)	(4 <i>c</i> )	0.0346(9)	0.4943(8)	0.2500
N	(4 <i>b</i> )	0.5000	0.0000	0.0000
As	(4 <i>a</i> )	0.0000	0.0100(4)	0.2500
Deviations from the ideal sites				
$\Delta_1 = 0.0286$ , $\Delta_2 = 0.0290$ , $\delta = 0.0171$ , $\gamma_1 = 0.0346$ , $\gamma_2 = 0.0057$ , $\lambda_1 = 0.0000$ , $\lambda_2 = 0.0100$				
Residual factors				
$R_p = 10.3\%$ , $R_{wp} = 15.7\%$ , reduced $\chi^2 = 1.42$ for 30 variables				

Note. Thermal parameters were taken from Table I.

where  $\phi$ ,  $\omega$ , and  $\varphi$  are the rotation angles about the *c*, *a'* (or *b'*), and *b*-axes, respectively. The calculated angles based on the refined results of the neutron data are listed below,

$$\begin{aligned} 305 \text{ K: } & \phi = 6.62^\circ, \quad \omega = 3.99^\circ, \quad \varphi = 5.02^\circ, \\ 15 \text{ K: } & \phi = 7.54^\circ, \quad \omega = 4.80^\circ, \quad \varphi = 6.46^\circ. \end{aligned}$$

The tilts are greater (or the structure is more distorted) at lower temperatures, as expected. The temperature dependence of the distortion implies that a phase transition to an undistorted cubic structure may occur above room temperature. Magnetic susceptibility measurements do suggest that such a transition takes place near 1025 K (8).

The interatomic distances are tabulated in Table IV. The N–Ca distances vary only slightly with an average value of  $\sim 2.40 \text{ \AA}$  (since the octahedron is nearly rigid); however, the As–N distances are spread over a large range of  $\sim 0.7 \text{ \AA}$ . An interesting observation is that those As–N distances which

are smaller than  $3.43 \text{ \AA}$  at 305 K become even smaller at 15 K, and those distances larger than  $3.47 \text{ \AA}$  at 305 K become even larger at 15 K. Therefore, it can be deduced that the As–N distance in the ideal undistorted perovskite is somewhere in between  $3.43$  and  $3.47 \text{ \AA}$ . The distortion shortens half

TABLE IV  
INTERATOMIC DISTANCES ( $\text{\AA}$ ) FOR  $\text{Ca}_3\text{AsN}$

	305 K	10 K	Number of atoms at that distance
N–Ca(1)	2.387(4)	2.398(3)	2
	2.416(4)	2.406(3)	2
N–Ca(2)	2.3944(3)	2.3957(2)	2
As–Ca(1)	3.083(2)	3.060(1)	2
	3.265(2)	3.256(2)	2
	3.432(2)	3.397(1)	2
	3.729(2)	3.787(2)	2
As–Ca(2)	3.158(3)	3.090(2)	1
	3.261(5)	3.216(3)	1
	3.477(5)	3.517(3)	1
	3.575(3)	3.633(2)	1

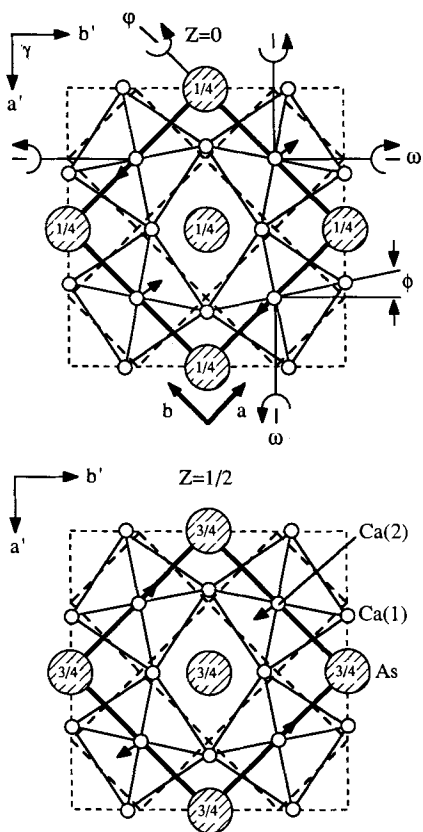


FIG. 6. The observed tilt of the anti-perovskite nitride  $\text{Ca}_3\text{AsN}$  with a view down the  $c$ -axis. The dotted lines are the doubled ideal cubic cell which contains eight nitrogen-centered calcium octahedra. The solid lines outline the distorted structure, and the unit cell is drawn by the bold solid lines. (Ca: small open circles, As: large hatched circles, N: not shown.) The waists, Ca(1), of the first and second layers of the octahedra are at approximately  $z = 0$  and  $z = \frac{1}{2}$ , respectively; the heights of the As atoms,  $\frac{1}{4}$  and  $\frac{3}{4}$ , are also marked; the tips, Ca(2), of the octahedra, which locate at  $z = \frac{1}{4}$  and  $\frac{3}{4}$  for the first and second layers of octahedra, respectively, tilt in the directions shown by the arrows. The tilt angles and directions of the octahedra about the  $c$ ,  $a'$  (or  $b'$ ), and  $b$ -axes are indicated by the arrowed semicircles and are labeled as  $\phi$ ,  $\omega$ , and  $\varphi$ , respectively.

of the As–N bonds to increase the overall stability of the structure while increasing the other half of the As–N bonds. At lower temperatures, this “disproportion” of the As–N bond lengths is greater as expected.

Distortions from cubic symmetry have

been reported in studies of other antiperovskite nitrides.  $\text{Cr}_3\text{AsN}$  exhibits a simple rotational distortion of the  $\text{Cr}_6\text{N}$  octahedra of the type  $a^0b^0c^-$ , as in  $\text{SrTiO}_3$  (13). The antiperovskite manganese nitrides,  $\text{Mn}_3\text{AN}$  with  $A = \text{As, Cu, Ga, Ge, Sb, . . .}$ , exhibit first and second order phase transitions from cubic to lower symmetry structures that are also presumably due to rotations of the  $\text{Mn}_6\text{N}$  octahedra (14).

In summary, the distorted structure of the anti-perovskite nitride  $\text{Ca}_3\text{AsN}$  has been solved. It belongs to the tilt system  $a^-a^-c^+$ , according to Glazer’s classification of distorted perovskites. For comparison, it will be interesting to solve the structure of the other distorted compound in this family of materials,  $\text{Ca}_3\text{PN}$ .

### Acknowledgments

Support of this work at Cornell University by the Office of Naval Research is greatly appreciated.

### References

1. H. D. MEGAW, “Crystal Structure: A Working Approach,” Saunders, Philadelphia (1971).
2. W. J. MERZ, *Phys. Rev.* **76**, 1221 (1949), and references therein.
3. T. MISTUI AND W. B. WESTPHAL, *Phys. Rev.* **124**, 1354 (1961), and references therein.
4. H. F. KAY AND P. C. BAILEY, *Acta Crystallogr.* **10**, 219 (1957).
5. K. KNOX, *Acta Crystallogr.* **14**, 583 (1961).
6. A. M. GLAZER, *Acta Crystallogr. Sect. B: Struct. Crystallogr. Cryst. Chem.* **28**, 3384 (1972).
7. A. M. GLAZER, *Acta Crystallogr., Sect. A: Cryst. Phys. Diffr. Theor. Gen. Crystallogr.* **31**, 756 (1975).
8. M. Y. CHERN, D. A. VENNOS, AND F. J. DiSALVO, *J. Solid State Chem.* **96**, 415–425 (1992).
9. A. C. LARSON AND R. B. VON DREELE, “Generalized Crystal Structure Analysis System,” LANSCE, MS-H805, Los Alamos National Laboratory, Los Alamos, NM 87545.
10. R. B. VON DREELE, J. D. JORGENSEN, AND C. G. WINDSOR, *J. Appl. Crystallogr.* **15**, 581 (1982).
11. C. J. HOWARD, *J. Appl. Crystallogr.* **15**, 615 (1982).
12. P. THOMPSON, D. E. COX, AND J. B. HASTINGS, *J. Appl. Crystallogr.* **20**, 79 (1982).
13. H. BOLLER, *Monatsch. Chem.* **99**, 2444 (1968).
14. M. BARBERON, R. MADAR, E. FRUCHART, G. LORTHOIR, AND R. FRUCHART, *Mater. Res. Bull.* **5**, 1 (1970).